ENGENHARIAS, TECNOLOGIA, GESTÃO E TURISMO
ENGINEERING, TECHNOLOGY, MANAGEMENT AND TOURISM
INGENIERÍA, TECNOLOGÍA, ADMINISTRACIÓN Y TURISMO

millenium 81

Millenium, 2(7), 81-90.

en

COMPORTAMENTO ELASTO-PLÁSTICO AO CORTE DE ESTRUTURAS FAVO-DE-MEL E AUXÉTICAS REFORÇADAS

ELASTO-PLASTIC SHEAR BEHAVIOR OF REINFORCED HONEYCOMB AND AUXETIC REENTRANT LATTICES

COMPORTAMIENTO ELASTO-PLÁSTICO AL CIZALLADURA DE ESTRUCTURAS PANAL Y AUGÉTICAS REFORZADAS

Vitor Carneiro[1]
José Meireles[1]

[1] *University of Minho, Braga, Portugal*

Vitor Carneiro - vitorhcarneiro@hotmail.com | José Meireles - meireles@dem.uminho.pt

Corresponding Author
Vitor Carneiro
Universidade do Minho
Largo do Paço
4704-553 Braga - Portugal
vitorhcarneiro@hotmail.com

RECEIVED: 27th March, 2018
ACCEPTED: 13th September, 2018

DOI: https://doi.org/10.29352/mill0207.07.00179

RESUMO

Introdução: Materiais auxéticos possuem um coeficiente de Poisson negativo. Ainda que a existência de auxéticos isotrópicos seja teoricamente possível, estes são inexistentes em estados naturais. Assim, tem havido um esforço para produzir auxéticos artificiais principalmente pelo design de favos de mel invertidos (reentrantes).
Objetivos: Este estudo explora novas estruturas reforçadas em favo de mel e auxéticas para melhorar o comportamento elasto-plástico estrutural em deformação de corte.
Métodos: A análise de elementos finitos (FEA) é usada para simular a carga de corte em estruturas reforçadas em favo de mel e auxéticas reentrantes, enquanto as tensões e deformações impostas são monitorizadas.
Resultados: A transformação auxética promove um aumento no módulo de corte, no entanto, gera deformações plásticas a valores mais baixos de deformação. No entanto, o efeito de fechamento de materiais auxéticos tende a reduzir a área de plasticidade afetada.
Conclusões: Neste estudo, é apresentada uma nova geração de estruturas reforçadas em favo de mel e auxética reentrante. Ainda que a transformação auxética gere deformação plástica para menores deformações de corte, é capaz de reduzir as áreas afetadas pela plasticidade e elevar a rigidez de corte.

Palavras-chave: Favo-de-mel; Auxético; Corte; Elastoplástico; Análise por elementos finitos.

ABSTRACT

Introduction: Auxetic materials possess a negative Poisson's ratio. Even though, the existence of isotropic auxetics is theoretically possible, they seem to be absent in natural states thus, there has been an effort to produce artificial auxetics mostly by the design of inverted (reentrant) honeycombs.
Objetives: This study explores a novel Reinforced Honeycomb Lattices and Auxetic Reentrant lattices to enhance structural elasto-plastic behaviour in shear deformation.
Methods: Finite element analysis (FEA) is used to simulate shear loading in Reinforced Honeycomb and Auxetic Reentrant lattices, while the imposed stress and strains are monitored.
Results: Auxetic transformation promotes an increase in shear modulus, however, it generates plastic strains at lower values of shear deformation. However, the closing effect of auxetic materials, tends to reduce the plastic affected area.
Conclusions: In this study, a novel generation of Reinforced Honeycomb and Auxetic Reentrant Lattices are presented. Even though, the auxetic transformation generates plastic strain for lower shear deformation regimes, it is able to reduce the areas affected by plasticity and elevate shear stiffness.

Keywords: Honeycomb; Auxetic; Shear; Elasto-Plastic; Finite element analysis.

RESUMEN

Introducción: Los materiales augéticos poseen un coeficiente de Poisson negativo. Aunque la existencia de augétios isotrópicos es teóricamente posible, parecen estar ausentes en los estados naturales, por lo tanto, se ha realizado un esfuerzo para producir augéticos artificiales principalmente mediante el diseño de panales invertidos.
Objetivos: Este estudio explora un enrejado de nido de abeja reforzado y enrejado reentrantes para mejorar el comportamiento estructural elasto-plástico en la deformación al cizalladura.
Métodos: Análisis de elementos finitos (FEA) se utiliza para simular la carga de cizallamiento en rejillas nido de abeja reforzadas y Reentrant augéticas, mientras que el estrés impuesto y las cepas se controlan.
Resultados: La transformación augética promueve un aumento en el módulo de cizalladura y genera deformaciones plásticas a valores más bajos de deformación por cizalladura. Sin embargo, el efecto de cierre de los materiales augéticos tiende a reducir el área plástica afectada.
Conclusiones: En este estudio, se presenta una nueva generación de enrejado de nido de abeja reforzado y rejillas augética reentrante. Apesar de que la transformación augética genera deformación plástica para regímenes de deformación de cizallamiento más bajo, es capaz de reducir las áreas afectadas por la plasticidad y elevar la rigidez a la cizalladura.

Palavras-clave: Nido de abeja; Augéticos; Cizalladura; Elasto-Plástica; Análisis de elementos finitos.

DOI: https://doi.org/10.29352/mill0207.07.00179

1. INTRODUCTION

Auxetic materials are characterized by an expansion or contraction in the transverse direction while they are axially tensioned or compressed, therefore, they possess a negative Poisson's ratio (Carneiro *et al*, 2013). While most common linear elastic isotropic materials tend to change their shape and have an isochoric deformation behavior, the referred materials are expected to keep their shape while experiencing extreme volume changes (Alderson & Alderson, 2007). Although this kind of deformation behavior may seem counterintuitive, it is supported by the thermodynamic balance of the classical Theory of Elasticity, which states that the Poisson's ratio has a lower limit of -1 and an upper limit of 0.5 and 1, respectively, for three-dimensional (Fung, 1965) and two-dimensional (Jasiuk & Chen, 1994) approaches.

Even though, the existence of isotropic auxetics is theoretically possible, they seem to be absent in natural states, being mostly found in anisotropic forms (e.g. (Voigt, 1882) (Gatt *et al*, 2015) (Keskar, 1992)). Thus, since the mid-1980's there has been an effort to produce artificial auxetics, first by the design of reticulated macrostructures (Almgren, 1985) and, later, by the manufacturing of the auxetic foams (Lakes, 1987). Since then, there were developed macrostructural models that show auxetic behavior (see for e.g. the reviews of (Carneiro *et al*, 2013) and (Greaves *et al*, 2011)), being the most common obtained by the inversion of lateral ribs of honeycombs to obtain two-dimensional reentrant structures and, on a three-dimensional approach, inverted tetrakaidecahedrons (Lakes, 1987).

It is expected that this kind of materials show enhanced specific mechanical properties such as high damping (Lim *et al*, 2013), higher hardness (Hu & Deng, 2015) and superior shear resistance (Greaves *et al*, 2011). However, in absolute terms given the cellular configuration that are used to produce these structures, their mechanical behavior may be compromised for many practical structural applications.

This study shows the transformation of Reinforced Honeycomb Lattices and some considerations for their transformations in Reinforced Auxetic Reentrant Lattices. Furthermore, their elasto-plastic behavior is characterized in terms of in-plane shear deformation to determine the advantage of the production of these lattices in their auxetic configuration.

2. METHODS

Regular honeycombs are characterized by a hexagonal configuration where all ribs have the same length. In order to transform this kind of structures into auxetic reentrant structures, the fundamental geometry must be changed, usually, to an arrangement where the horizontal ribs (H) have a superior dimension than the vertical ribs (L), generally using the proportion of H=2L (Figure 1 – a).

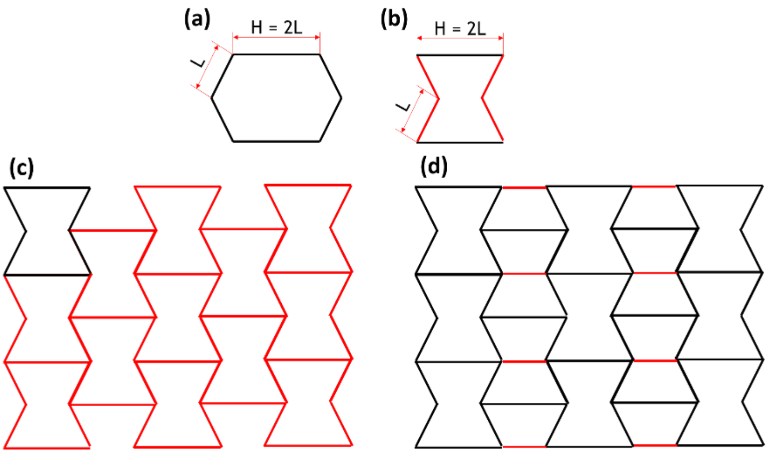

Figure 1. General procedure to model Reinforced Auxetic Reentrant Lattices:
a) original Honeycomb; b) Rib inversion; c) Cell assembly; d) Adding of reinforcement struts.

By the inversion of the vertical ribs (Figure 1 – b), it is possible to transform the defined Honeycomb into an Auxetic Reentrant geometry. By the assembly of these geometries (Figure 1 – c), a lattice configuration may be obtained. Finally, Reinforced Auxetic Reentrant Lattices are proposed by this study and may be achieved by the addition of horizontal struts in every other row of unitary cells (Figure 1 – d).

A similar procedure may be applied to the Honeycomb (Figure 2 – a), by eliminating the rib inversion step and proceed directly to the assembly phase (Figure 2 – b). The Reinforced Honeycombs Lattices that are proposed by this study, may be obtained by the assembly of horizontal struts in the manner that was referred in the previous procedure (Figure 2 – c).

Carneiro, V. & Meireles, J. (2018).
Elasto-plastic shear behavior of reinforced honeycomb and auxetic reentrant lattices. *Millenium, 2*(6), 81-90.
DOI: https://doi.org/10.29352/mill0207.07.00179

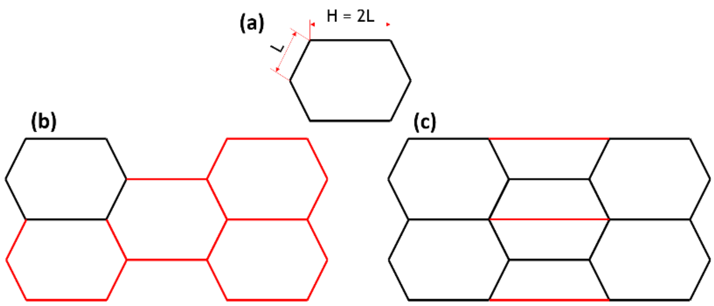

Figure 2. General procedure to model Reinforced Honeycomb Lattices:
a) Initial Honeycomb; b) Cell assembly; c) Adding of reinforcement struts.

Using the both procedures for Reinforced Reentrant Auxetic and Honeycomb Lattices, there were obtained the two-dimensional structures shown in Figures 3. The overall dimensions of the design structures are presented in Table 1.

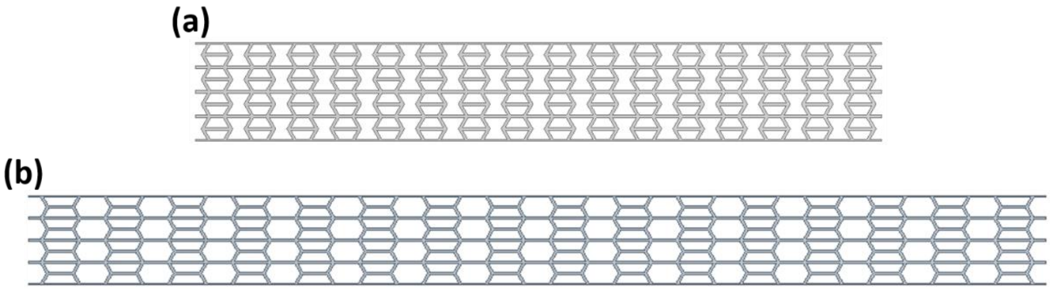

Figure 3. Novel reinforced structure: a) auxetic reentrant and b) honeycomb.

Table 1 – General dimensions of the modeled lattices.

<table>
<tr><td rowspan="5">Unitary Cells</td><td rowspan="3">Distance Dimensions [mm]</td><td>H – Horizontal Ribs</td><td>40</td></tr>
<tr><td>L – Vertical Ribs</td><td>20</td></tr>
<tr><td>B – Rib Thickness</td><td>4</td></tr>
<tr><td rowspan="2">Angular Dimensions [°]</td><td>Auxetic Reentrant</td><td>30</td></tr>
<tr><td>Honeycomb</td><td>120</td></tr>
<tr><td rowspan="3">Final Lattices</td><td>Height [mm]</td><td colspan="2">138</td></tr>
<tr><td rowspan="2">Length [mm]</td><td>Auxetic Reentrant</td><td>960</td></tr>
<tr><td>Honeycomb</td><td>1600</td></tr>
</table>

The elasto-plastic behavior of the modeled structures when subjected to a shear effort were estimated by use of FE analysis, recurring to a static structural routine of ANSYS 17. Fundamentally, the defined models were fixed in their lower face, while their upper face is subjected to a Displacement of 5 [mm] in the horizontal direction (XX axis), being these boundary conditions represented in Figure 4. In terms of Apparent Shear Strain (γ), the applied displacement corresponds to 0.035, enough to characterize the local deformations within the plastic regime without entering in severe plastic deformation. This corresponds to a simulation of these structures in practical situations where small permanent dislocations are allowed within their life span.

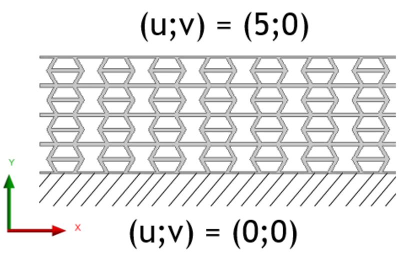

Figure 4. Representation of boundary conditions used in the FE analysis.

To characterize these elastic, local plastic and the corresponding transition regime, an Aluminum with a Bilinear Isotropic Hardening behavior was selected as the base material for the FE routines. The input conditions for the numerical procedures are shown in Table 2, being that the main outputs of the simulation are the correspondent Reaction Forces and Local Plastic Strain values and locations. The fundamental material properties were determined from previous tensile tests (Fig. 5 – a). Details of the mesh may be observed in Fig.5-b, where the elements (Table 2) are smoothly discretized to obtain smooth simulation results.

Table 2 - FEA input conditions.

Material	Aluminum (Bilinear Isotropic Hardening)	Young's Modulus [GPa]	71
		Poisson's Ratio [-]	0.33
		Yield Strength [MPa]	230
		Tangent Modulus [GPa]	0.5
Contacts	Type	Frictionless	
	Formulation	Pure Penalty	
Mesh	Element Type	SHELL181 – 1 [mm] element size	
	Description	Rectangular - 4 Noded	
Boundary Conditions	Upper Face	{u=5;v=0} [mm]	
	Lower Face	{u=0;v=0} [mm]	
Solver	Sparse direct equation solver		

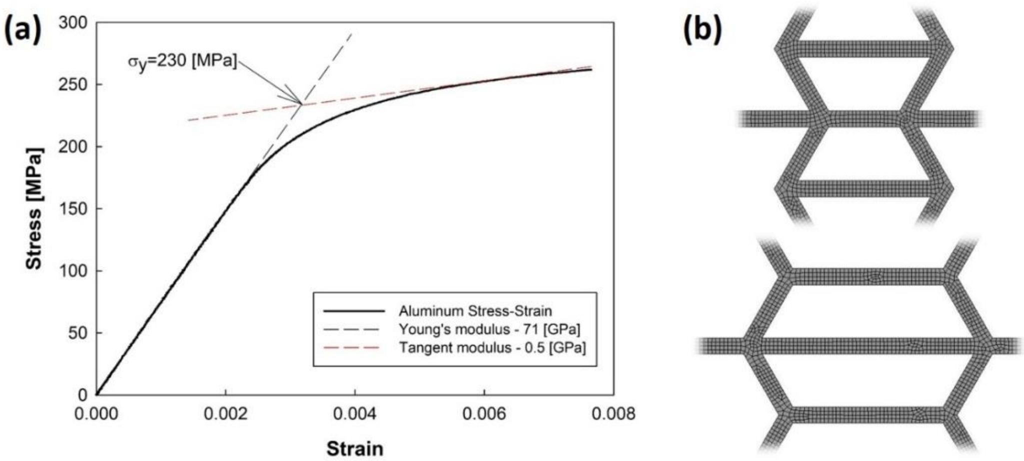

Figure 5. a) aluminum tensile behavior; b) meshing details.

3. RESULTS AND DISCUSSION

The Reaction Forces and Displacements from the numerical results are presented in Figure 6, by the calculation of the instant values of Apparent Shear Stress (τ) and Strain (γ).

DOI: https://doi.org/10.29352/mill0207.07.00179

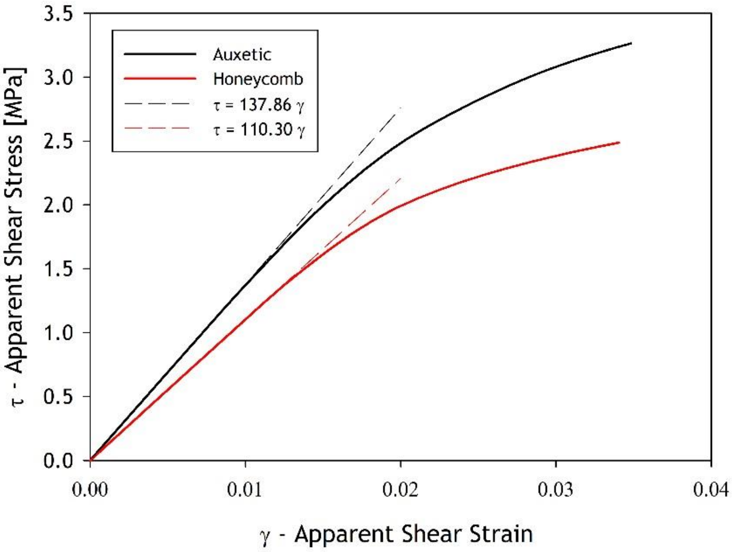

Figure 6. Resultant Apparent Shear Stress-Strain curves.

The dashed lines in Figure 6 are linear regressions that follow the slope of the linear elastic domain of the simulated models. Fundamentally, these values of slope represent the Apparent Shear Modulus (G*), and it maybe concluded that the transformation of the Reinforced Honeycombs Lattices to a Reinforced Auxetic Reentrant configuration, generates an elevation in this constant.

Comparing the results with theories (Fig.7) that describe the elastic behavior of cellular structures (e.g. honeycombs), it is shown that the reinforcement are able to generate an increase in shear stiffness. Reinforced Honeycombs display a substantial increase in Apparent Shear Modulus relatively to the theories of Gibson (1982) and Meraghni (1999). This implies that rib flexing does not completely dominate the deformation mechanism and the rib thickness influences the overall mechanical response in shear. This is further proved by the proximity of the results with the thick honeycomb theory described by Malek (2015). Additionally, it is shown that the transformation into Reinforced Auxetics is able to further elevate the shear stiffness.

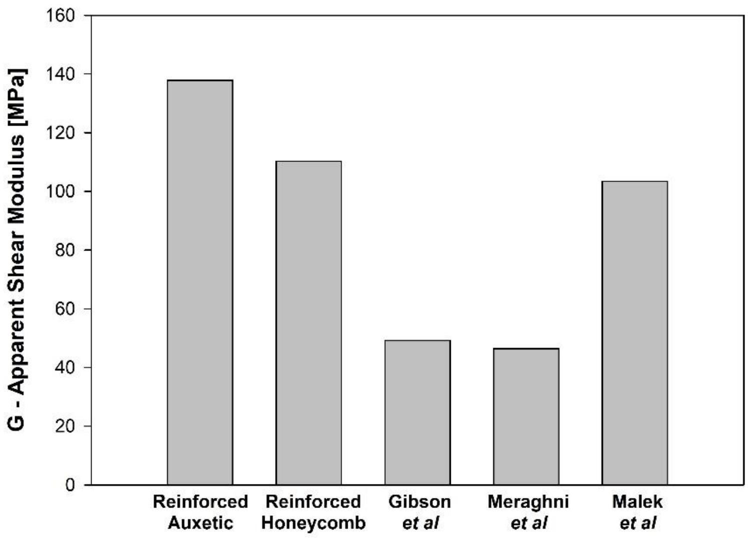

Figure 7. Comparison of the results with honeycomb elastic theories.

Even though, the elastic behavior of these structures due to their cellular morphology do not follow the behavior of the classical Theory of Elasticity, a parallel may be found to justify this increase of this elastic constant. Given that the Shear

DOI: https://doi.org/10.29352/mill0207.07.00179

Modulus (G) of an elastic isotropic solid is related to the Young's Modulus and Poisson's ratio by Equation 1 (Timoshenko & Goodier, 1951), it is expected that this constant increases for low values of Poisson's ratio as plotted in Figure 8.

$$G = \frac{E}{2(1+\nu)} \qquad (1)$$

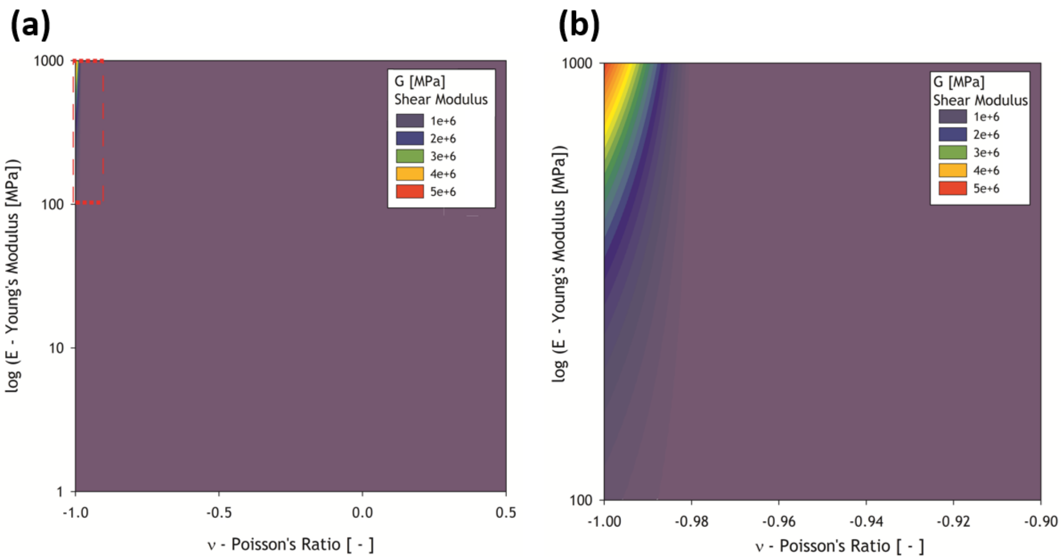

Figure 8. Linear elastic isotropic Shear Modulus as a function of the Young's Modulus and Poisson's ratio.

By the normalization of the Shear Modulus to the Young's modulus (G/E) (represented in Figure 9) it may be further observed that a general decrease in the Poisson's ratio will generate an increase in the Normalized Shear Modulus. Thus, these theory is able to predict an expected increase in this elastic constant as shown by the numerical results.

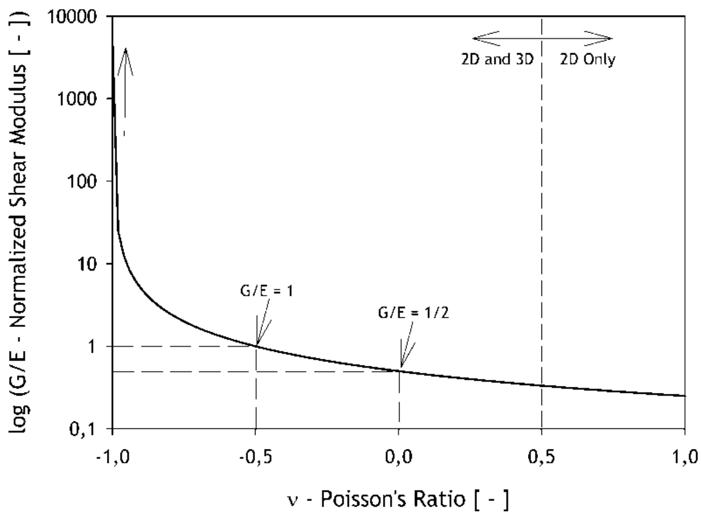

Figure 9. Normalized Shear Modulus (G/E) as a function of Poisson's ratio.

Further increasing the Apparent Shear Strain, the curves in Figure 6 tend to deviate from the linear regression, meaning that plastic deformation occurs and the overall deformation of the lattices is ruled by an elasto-plastic regime. Figure 10 shows the instant values of Maximum Normal Plastic Strain (ε^P) resultant from the numerical results, where it may be observed that Plastic Strain is verified at lower Apparent Shear Strain in Reinforced Auxetic Reentrant Lattices and even the elevation rate of Plastic Strain is more elevated.

Carneiro, V. & Meireles, J. (2018).
Elasto-plastic shear behavior of reinforced honeycomb and auxetic reentrant lattices. *Millenium, 2*(6), 81-90.
DOI: https://doi.org/10.29352/mill0207.07.00179

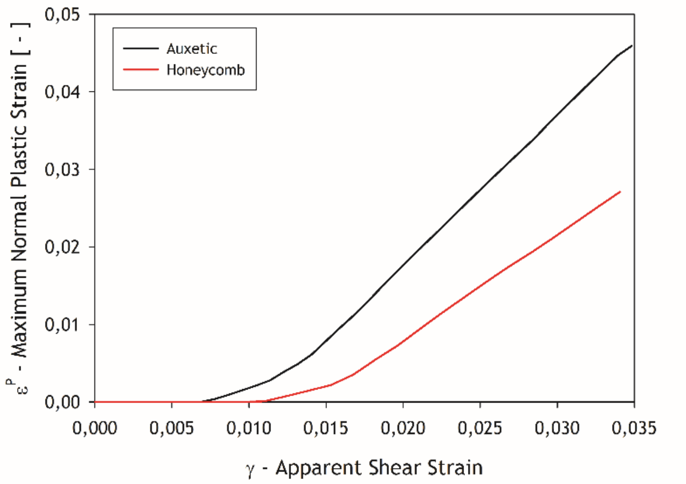

Figure 10. Maximum Normal Plastic Strain as a function of Apparent Shear Strain.

This progression in the increase of Maximum Normal Plastic Strain is further detailed in Figures 11 and 12, where several stages of Apparent Shear Strain are portrayed. From these figures it is verified that stress concentration generates Plastic Strain in the vertical ribs at lower Apparent Shear Strain for Reinforced Auxetic Reentrant Lattices (Figure 11). However, observing Figure 12, it may be stated that the Affected Plastic Area tends to be wider in the Reinforced Honeycomb Lattices and form Plastic Hinges in the horizontal ribs at lower Apparent Shear Strain. This last fact is suggested to contribute to the lowering of Apparent Shear Stress in Reinforced Honeycomb Lattices show in Figure 6, and thus contributing for the lower performance of these structures when subjected to shear loading.

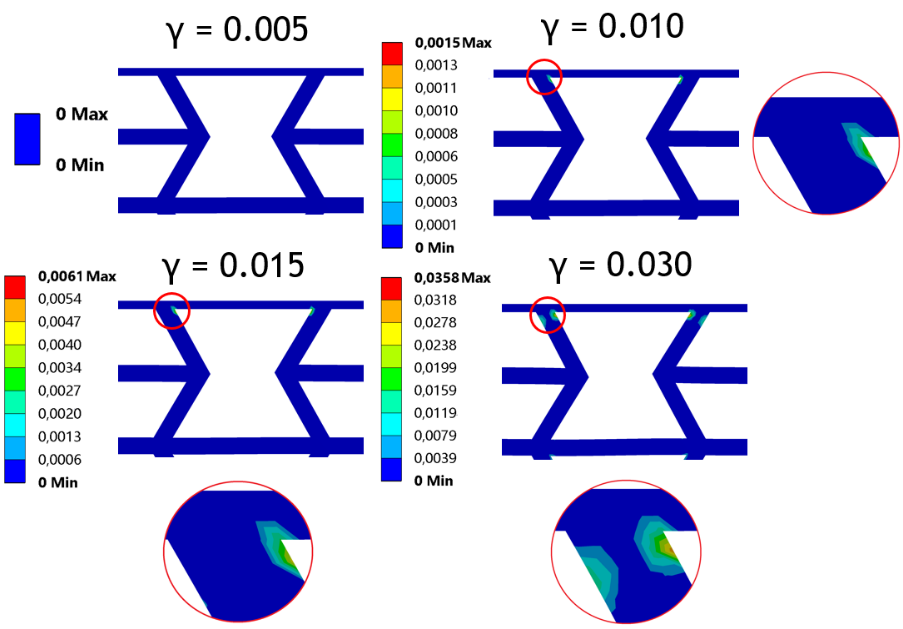

Figure 11. Detail progression of Plastic Strain in Reinforced Auxetic Reentrant Lattices.

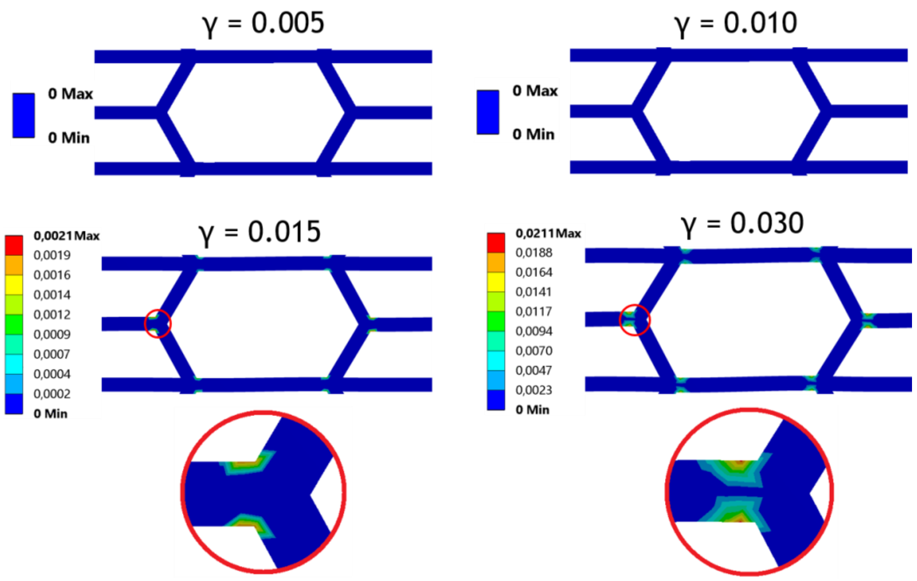

Figure 12. Detail progression of Plastic Strain in Reinforced Honeycomb Lattices.

CONCLUSIONS

In this study, a novel generation of Reinforced Honeycomb and Auxetic Reentrant Lattices are presented, while their elasto-plastic behavior due to shear loading is explored. Considering the overall results and discussion of the performed work, the following conclusions were drawn:

(i) Apparent Shear Modulus is higher in Reinforced Auxetic Reentrant Lattices than in Reinforced Honeycomb Lattices with the same cell dimensions;

(ii) Plastic Strain is verified at lower Apparent Shear Strain for Reinforced Auxetic Reentrant Lattices;

iii) Local Maximum Plastic Strain is higher in Reinforced Auxetic Reentrant Lattices, however, Reinforced Honeycomb Lattices display a wider Plastic Affected Zone;

iv) Development of Plastic Hinges occurs at lower Apparent Shear Strain for Reinforced Honeycomb Lattices, and overall this effect diminishes their performance in shear loading when compared with Reinforced Auxetic Reentrant Lattices.

ACKNOWLEDGEMENTS

This research was supported by the project iRAIL Innovation in Railway Systems and Technologies Doctoral Programme funds and by national funds through FCT - Portuguese Foundation for Science and Technology and was developed on the aim of the Doctoral grant PD/BD/114096/2015.

REFERENCES

Alderson, A., & Alderson K.L. (2007). Auxetic Materials. Proceedings of the Institution of Mechanical Engineers Part G Journal of Aerospace Engineering, 221, 565-575. https://doi.org/10.1243/09544100JAERO185

Almgren, R.F. (1985). An isotropic three-dimensional structure with Poisson's ratio – 1. Journal of Elasticity, 15, 427-430.

Carneiro, V.H., Meireles J., & Puga H. (2013). Auxetic Materials – A Review. Materials Science – Poland, 31(4), 561-571. Retrieved from: https://link.springer.com/article/10.2478/s13536-013-0140-6.

Fung, Y. (1965). Foundations of solid mechanics. New Jersey, USA: Prentice Hall.

Gatt, R., Wood, M.V., Gatt, A., Formosa, C., Azzopardi, K.M., Casha, A., Agius, T.P., … Grima, J.N. (2015). Negative Poisson’s ratios in tendons: An unexpected mechanical response. Acta Biomaterialia, 24, 201-208. https://doi.org/10.1016/j.actbio.2015.06.018

Gibson, L.J., Ashby, M.F., Schajer, G.S., & Robertson, C.I. (1982). The mechanics of two-dimensional materials. Proceedings of the Royal Society A, 382, 25-42. https://doi.org/10.1098/rspa.1982.0087

Greaves, G.N., Greer, A.L., Lakes, R.S., & Rouxel, T. (2011). Poisson’s ratio and modern materials. Nature Materials, 10 (11), 823-837. Retrieved from: https://www.nature.com/articles/nmat3134.

Carneiro, V. & Meireles, J. (2018).
Elasto-plastic shear behavior of reinforced honeycomb and auxetic reentrant lattices. *Millenium, 2*(6), 81-90.
DOI: https://doi.org/10.29352/mill0207.07.00179

Hu, L.L., & Deng, H. (2015). Indentation resistance of the re-entrant hexagonal honeycombs with negative Poisson’s ratio. Materials Research Innovations, 19, 441-445. https://doi.org/10.1179/1432891715Z.0000000001588

Jasiuk, I., Chen, J., & Thorpe, M.F. (1994). Moduli of Two Dimensional Materials With Polygonal and Elliptical Holes. Applied Mechanics Reviews, 47, 18-28. https://doi.org/10.1115/1.3122813

Keskar, N.R., & Chelikowsky, J.R. (1992). Negative Poisson ratios in crystalline SiO2 from first-principles calculations. Nature, 358, 222-224. https://doi.org/10.1038/358222a0

Lakes, R.S. (1987). Foam Structures with a Negative Poisson's Ratio. Science, 235, 1038-1040. https://doi.org/10.1126/science.235.4792.1038

Lim, T.C., Cheang, P., & Scarpa, F. (2013). Wave motion in auxetic solids. Physica Status Solidi B, 251, 388-396. https://doi.org/10.1002/pssb.201384238

Malek, S., & Gibson, L. (2015). Effective elastic properties of periodic hexagonal honeycombs. Mechanics of Materials, 91, 226-240. http://dx.doi.org/10.1016/j.mechmat.2015.07.008

Merhagni, F., Desrumaux, F., & Benzeggagh, M.L. (1999). Mechanical behaviour of cellular core for structural sandwich panels. Composites Part A: Applied Science and Manufacturing, 30, 767-779.

Timoshenko, S., & Goodier, J.N. (1951). Theory of Elasticity. New York, USA: McGraw-Hill.

Voigt, W. (1882). Allgemeine Formeln für die Bestimmung der Elasticitätsconstanten von Krystallen durch die Beobachtung der Biegung und Drillung von Prismen. Annalen der Physik, 252, 273-321. https://doi.org/10.1002/andp.18822520607